NASA TECHNICAL NOTE

NASA TN D-2341

NASA TN D-2341

A NUMERICAL METHOD FOR THE DESIGN OF CAMBER SURFACES OF SUPERSONIC WINGS WITH ARBITRARY PLANFORMS

by Harry W. Carlson and Wilbur D. Middleton

Langley Research Center
Langley Station, Hampton, Va.

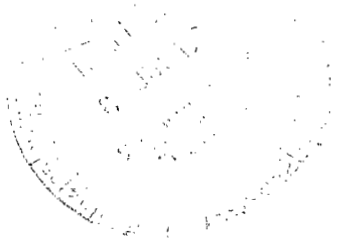

NATIONAL AERONAUTICS AND SPACE ADMINISTRATION • WASHINGTON, D. C. • JUNE 1964

A NUMERICAL METHOD FOR THE DESIGN OF CAMBER SURFACES OF SUPERSONIC WINGS WITH ARBITRARY PLANFORMS

By Harry W. Carlson and Wilbur D. Middleton

Langley Research Center
Langley Station, Hampton, Va.

NATIONAL AERONAUTICS AND SPACE ADMINISTRATION

For sale by the Office of Technical Services, Department of Commerce,
Washington, D. C. 20230 -- Price $0.50

A NUMERICAL METHOD FOR THE DESIGN OF CAMBER SURFACES OF SUPERSONIC WINGS WITH ARBITRARY PLANFORMS

By Harry W. Carlson and Wilbur D. Middleton
Langley Research Center

SUMMARY

This report presents a numerical method based on linearized theory which allows the determination of camber surfaces corresponding to certain specified load distributions for wings of arbitrary planform, and shows how these results may be combined with existing methods of selecting optimum combinations of loadings. To illustrate the application of the method and to point out certain features of wings with curved or cranked leading edges, a set of examples is presented. The principal checks on the precision of the method are made through comparisons with results for arrow- or delta-wing planforms by using established methods.

INTRODUCTION

For highly swept wings of arrow planform, theoretical studies such as that of reference 1 have indicated large potential performance benefits resulting from warping of the wing surface to produce an optimum or near-optimum load distribution and thus reduce the drag at a specified lift coefficient. Description of the camber surface necessary to support specified loadings for arrow wings may be obtained by using methods reported in the literature, for example, that of reference 2. Optimum combinations of component loadings designed to minimize drag at a given total lift coefficient may be found in the manner described in reference 3. Experimental investigations (refs. 4 and 5) of wings designed by using these theoretical concepts have shown that substantial portions of the theoretical benefits may indeed be achieved in practice, provided that realistic restraints are placed on the severity of camber surface slopes and on allowable local pressures.

Linearized theory integral equations for calculating the streamwise gradients of a wing camber surface for a given load distribution (ref. 6) are not restricted in application to the arrow planforms previously discussed, and with the development of high-speed electronic computing machines, it is possible to devise design methods for wings of rather arbitrary planform which may employ curved leading and trailing edges. This report presents a numerical method which allows the determination of camber surfaces corresponding to certain specified load distributions for wings of arbitrary planform, and shows how

these results may be combined with existing methods of selecting optimum combinations of loadings. To illustrate the application of the method and to point out certain features of wings with curved or cranked leading edges, a set of examples are presented. The principal checks on the validity of the method are made through comparisons with results for arrow- or delta-wing planforms using the established methods of reference 2.

SYMBOLS

A_i	load strength factor
$A(L,N)$, $A(L^*,N^*)$	leading-edge grid element weighting factor (See eqs. (6) and (12).)
b	wing span
$B(L^*,N^*)$	trailing-edge grid element weighting factor (See eq. (12).)
c	local wing chord
c_d	section drag coefficient
c_m	section moment coefficient
c_l	section lift coefficient
C_D	drag coefficient
$C_{D,i}$	drag coefficient of ith loading, $\frac{1}{2}C_{D,ii}$
$C_{D,ij}$	drag coefficient of interference between ith and jth component loadings
$C_D/\beta C_L^2$	drag-due-to-lift factor
C_L	lift coefficient
$C_{L,i}$	lift coefficient of ith loading
C_m	moment coefficient about $x = 0$ line referenced to wing length
C_p	pressure coefficient
ΔC_p	lifting pressure coefficient

$\Delta C_{p,i}$	lifting pressure coefficient of ith loading
k	constant
l	overall length of wing measured in streamwise direction
L,N	designation of influencing grid elements (See fig. 2.)
L*,N*	designation of field-point grid elements (See fig. 2.)
M	Mach number
R	influence function (See eq. (3).)
$\overline{R}$	average value of influence function within a grid element (See eq. (8).)
S	wing area
X,Y,Z	Cartesian coordinate system, X-axis streamwise
x,y,z	distance along X-, Y-, and Z-axes, respectively
x'	distance from wing leading edge measured in x-direction
z_c	camber surface ordinate
$\beta = \sqrt{M^2 - 1}$	
λ	Lagrange multiplier
ξ,η	dummy variables of integration for x and y, respectively
τ	designates a region of integration bounded by the wing planform and the fore Mach cone from the point x,y

Subscripts:

1,2,3	designates constants corresponding to specific loadings
i,j	ith and jth component loadings
min	minimum
max	maximum
n	number of component loadings
le	value of quantity along wing leading edge
te	value of quantity along wing trailing edge

NUMERICAL CALCULATION METHOD

Camber Surface for a Given Loading

A typical wing planform described by a rectangular Cartesian coordinate system is illustrated in figure 1. For a wing of zero thickness lying essentially in the $z = 0$ plane, linearized theory for supersonic flow defines the wing surface shape necessary to support a specified lift distribution by the integral equation

$$\frac{\partial z_c}{\partial x}(x,y) = \frac{-\beta}{4}\Delta C_p(x,y) + \frac{1}{4\pi}\int d\xi \oint_{\tau} \frac{(x - \xi)\,\Delta C_p(\xi,\eta)\,d\eta}{(y - \eta)^2\sqrt{(x - \xi)^2 - \beta^2(y - \eta)^2}} \qquad (1)$$

which is a slightly modified form of equation (77a) of reference 6. The region of integration τ extends over the wing planform within the fore Mach cone from the field point x,y as shown by the shaded area in figure 1. The integral on the right-hand side of equation (1) gives the appearance of being

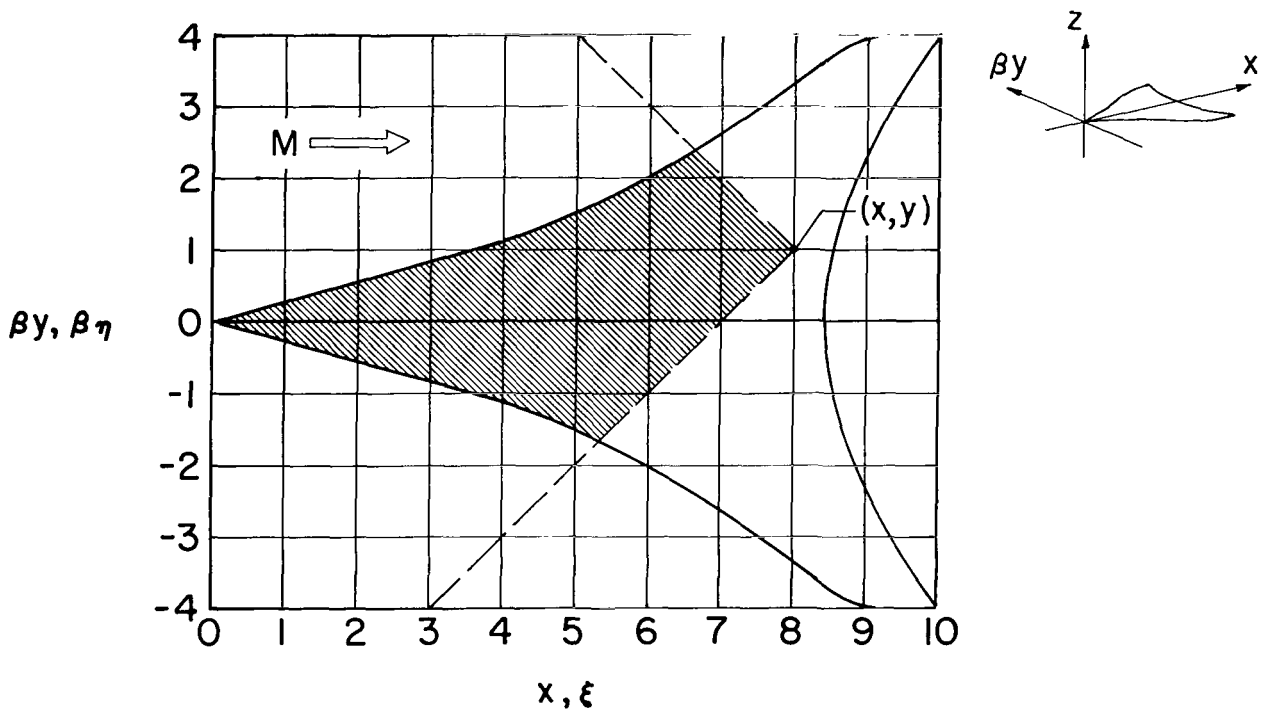

Figure 1.- Cartesian coordinate system.

improper and divergent because of the singularity at $\eta = y$ within the region of integration. This integrand is, however, the limiting form in the $z = 0$ plane of a more general integrand that arises from lifting surface theory and does not have a singularity at $\eta = y$ when $z \neq 0$. Consequently, the integral

can be treated according to the concept of the generalization of the Cauchy principal value, which is discussed and explained in section 3 of reference 7 and also in reference 6. The integral is thus generally found to be convergent at points x,y on a wing surface, although regions of nonconvergence exist if there are values of y for which the spanwise derivative of the chordwise integral

$$\frac{\partial}{\partial \eta} \int_{\xi_{le}}^{x-\beta|y-\eta|} \frac{(x - \xi)\, \Delta C_p(\xi,\eta)}{\sqrt{(x - \xi)^2 - \beta^2(y - \eta)^2}}\, d\xi$$

is not single valued at $\eta = y$. These regions of nonconvergence, however, do not invalidate results over the remainder of the wing surface.

For the purposes of this study, equation (1) will be rewritten in the form

$$\frac{\partial z_c}{\partial x}(x,y) = \frac{-\beta}{4} \Delta C_p(x,y) + \frac{\beta}{4\pi} \oint d\xi \oint_{\tau} R(x-\xi,y-\eta)\, \Delta C_p(\xi,\eta)\, d\beta\eta \qquad (2)$$

where the function R is defined as

$$R(x-\xi,y-\eta) = \frac{x - \xi}{\beta^2(y - \eta)^2\sqrt{(x - \xi)^2 - \beta^2(y - \eta)^2}} \qquad (3)$$

and may be thought of as an influence function relating the local loading at point ξ,η to its influence in determining the necessary slope at downstream point x,y.

In order to replace the indicated integration in equation (2) by a numerical summation, it is first necessary to introduce a grid system superimposed over the Cartesian coordinate system used in describing the wing planform as shown in figure 2. (This sketch is illustrative only; in application many more grid elements would be employed.) The numbers assigned to L and N identify the spaces in the grid which replace the element of integration $d\xi,d\beta\eta$. The starred values of L and N identify the space or element associated with and immediately ahead of the field point x,y; L^* is numerically equal to x and N^* is numerically equal to βy, where x and βy take on only integer values. The region of integration, originally bounded by the wing leading edge and the Mach lines, now consist of a set of grid elements approximating that region as shown by the shaded area in the example of figure 2.

The contribution of each element of the wing L,N to the local slope at $x,\beta y$ may be written as:

$$\frac{\partial z_c}{\partial x}(x,y) = \frac{\beta}{4\pi} \bar{R}(L^*-L,N^*-N)\, A(L,N)\, \Delta C_p(L,N) \qquad (4)$$

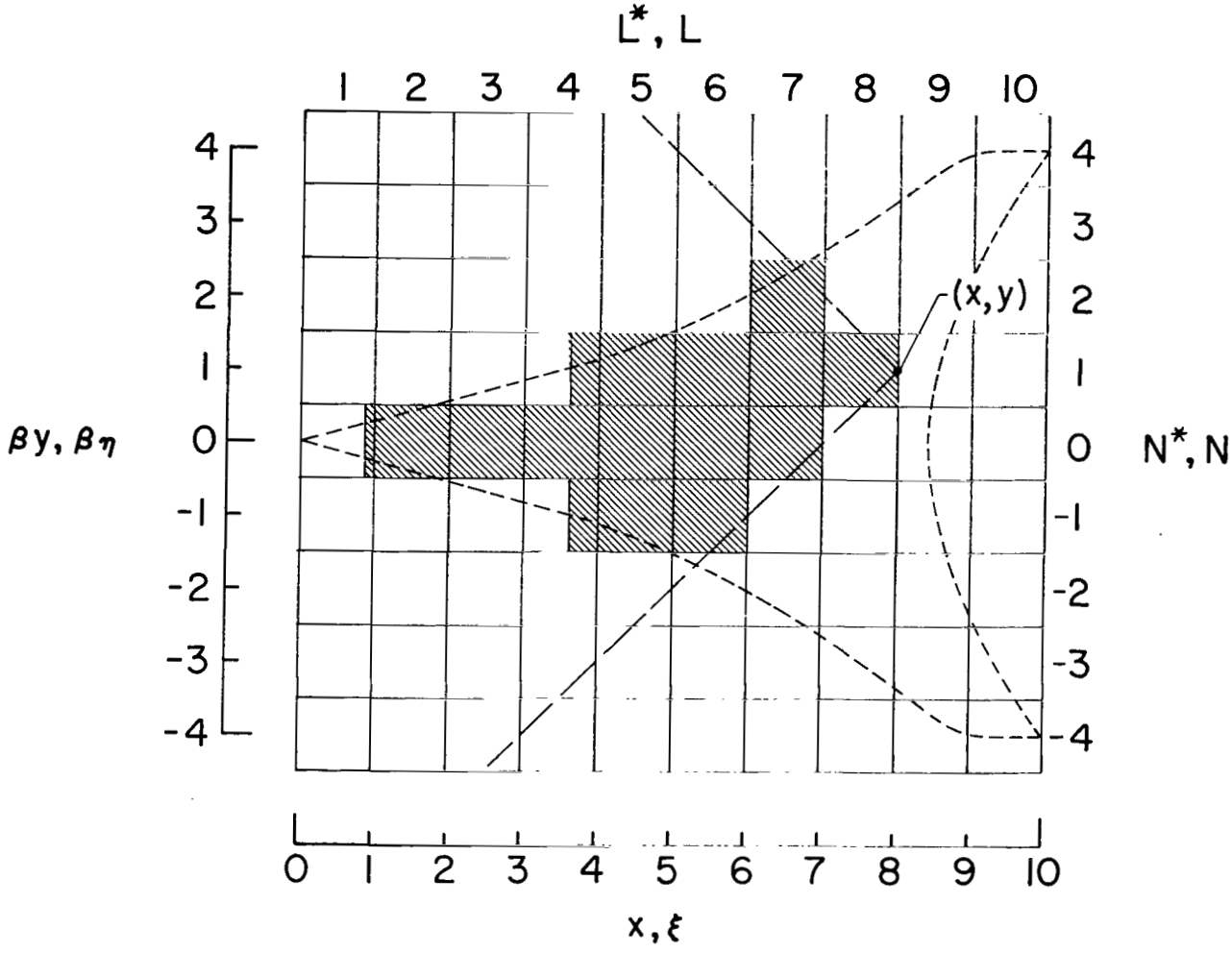

Figure 2.- Grid coordinate system.

with the factor $\bar{R}$ representing an average value within the element of the function $R(x-\xi,y-\eta)$. The value of this factor may be found from the integral

$$\bar{R}(L^*-L,N^*-N) = \frac{1}{\Delta\xi\,\Delta\beta\eta}\int_{\xi_1}^{\xi_2} d\xi \int_{\beta\eta_1}^{\beta\eta_2} \frac{(x-\xi)}{\beta^2(y-\eta)^2\sqrt{(x-\xi)^2-\beta^2(y-\eta)^2}}\, d\beta\eta \qquad (5)$$

in which the integration extends over one grid element. Since it has been observed that the integrand is relatively insensitive to variations in ξ, as an approximation the $\bar{R}$ function may be written as

$$\bar{R}(L^*-L,N^*-N) = \frac{1}{\Delta\beta\eta}\int_{\beta\eta_1}^{\beta\eta_2} \frac{(L^*-L+0.5)}{\beta^2(y-\eta)^2\sqrt{(L^*-L+0.5)^2-\beta^2(y-\eta)^2}}\, d\beta\eta \qquad (6)$$

with $(L^* - L + 0.5)$ representing the value of $x - \xi$ at the midpoint of the element. On integration the expression takes the form

$$\bar{R}(L^*-L,N^*-N) = \frac{(L^* - L + 0.5)\sqrt{(L^* - L + 0.5)^2 - \beta^2(y - \eta)^2}}{(L^* - L + 0.5)^2\beta(y - \eta)} \Bigg|_{\beta\eta_1}^{\beta\eta_2} \tag{7}$$

and with $\beta y = N^*$, $\beta\eta_1 = N - 0.5$, and $\beta\eta_2 = N + 0.5$ (see fig. 2), the influence factor $\bar{R}$ becomes

$$\bar{R}(L^*-L,N^*-N) = \frac{\sqrt{(L^* - L + 0.5)^2 - (N^* - N - 0.5)^2}}{(L^* - L + 0.5)(N^* - N - 0.5)} - \frac{\sqrt{(L^* - L + 0.5)^2 - (N^* - N + 0.5)^2}}{(L^* - L + 0.5)(N^* - N + 0.5)} \tag{8}$$

A graphical representation of this factor is shown in figure 3. Note the rather small variations of the factor in the x- or L-direction contrasted with the

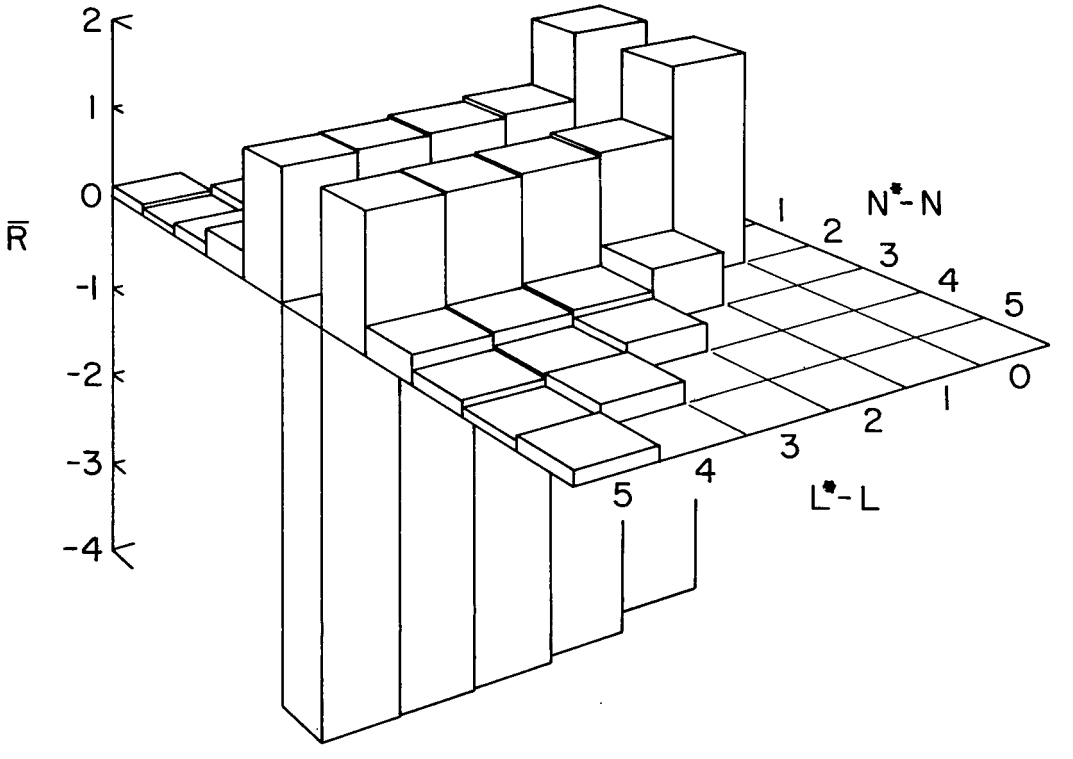

Figure 3.- Distribution of $\bar{R}$ function.

drastic variations in the y- or N-direction. For a given $L^* - L$ set of elements, the sum of the $\bar{R}$ values is zero, the single negative value at $N^* - N = 0$ balancing all the others. At $L^* - L = 0$ where there is only one element in the summation region, the $\bar{R}$ value of the element is zero.

The $A(L,N)$ term in equation (4) is a weighting factor which eliminates the necessity of accepting or rejecting complete block elements and thus permits a better definition of the wing leading-edge shape, which has been found to be extremely critical. The factor $A(L,N)$ takes on values from 0 to 1 given by

$$\left.\begin{aligned} A(L,N) &= 0 && \left(L - x_{le} \leqq 0\right) \\ A(L,N) &= L - x_{le} && \left(0 < L - x_{le} < 1\right) \\ A(L,N) &= 1 && \left(L - x_{le} \geqq 1\right) \end{aligned}\right\} \tag{9}$$

Desired values of lifting pressure coefficient $\Delta C_p(L,N)$ are assigned to each space or element of the grid. The pressure may vary from element to element, but is assumed to be constant within a given element. Values of $\Delta C_p(L,N)$ may be tabulated for each of the elements or more conveniently may be expressed in equation form.

The wing surface slope at a point represented by L^* and N^* may now be found by a summation of the contributions of each of the elements within the influencing region which is expressed as:

$$\frac{\partial z_c}{\partial x}(L^*,N^*) = \frac{-\beta}{4} \Delta C_p(L^*,N^*) + \frac{\beta}{4\pi} \sum_{N=N_{min}}^{N=N_{max}} \sum_{L=1+\left[x_{le}\right]}^{L=L^*-\left|N^*-N\right|} \bar{R}(L^*-L,N^*-N)\, A(L,N)\, \Delta C_p(L,N) \tag{10}$$

The vertical lines as used in $\left|N^* - N\right|$ designate the absolute value of the enclosed quantity and the brackets in $\left[x_{le}\right]$ designate the whole number part of the quantity. The initial summation with respect to L is made only when

$$L^* - \left|N^* - N\right| \geqq 1 + \left[x_{le}\right]$$

The z-ordinate of the wing surface at station $x = L^*$ for a given semispan station $y = \frac{N^*}{\beta}$ may be found by a chordwise summation of the local slopes given by

$$z_c(x,y) = \sum_{L^*=1+\lceil x_{le} \rceil}^{L^*=x} A(L^*,N^*) \frac{\partial z_c}{\partial x}(L^*,N^*) \tag{11}$$

where x takes on only integer values. Equation (11) gives a zero camber ordinate along the wing leading edge. In reference 2 it is pointed out that such an arbitrary choice of the leading-edge z_c-value does not influence the theoretical wing characteristics.

Section lift, drag, and pitching-moment coefficients at semispan station $y = \frac{N^*}{\beta}$ may be evaluated by the following summations:

$$c_l = \frac{1}{c} \sum_{L^*=1+\lceil x_{le} \rceil}^{L^*=1+\lceil x_{te} \rceil} \Delta C_p(L^*,N^*)\, A(L^*,N^*)\, B(L^*,N^*) \tag{12}$$

$$c_d = \frac{1}{c} \sum_{L^*=1+\lceil x_{le} \rceil}^{L^*=1+\lceil x_{te} \rceil} \frac{\partial z}{\partial x}(L^*,N^*)\, \Delta C_p(L^*,N^*)\, A(L^*,N^*)\, B(L^*,N^*) \tag{13}$$

$$c_m = \frac{1}{c^2} \sum_{L^*=1+\lceil x_{le} \rceil}^{L^*=1+\lceil x_{te} \rceil} (L^* - 0.5)\, \Delta C_p(L^*,N^*),\, A(L^*,N^*)\, B(L^*,N^*) \tag{14}$$

where

$$\left.\begin{aligned}
A(L^*,N^*) &= 0 && \left(L^* - x_{le} \leqq 0\right) \\
A(L^*,N^*) &= L^* - x_{le} && \left(0 < L^* - x_{le} < 1\right) \\
A(L^*,N^*) &= 1 && \left(L^* - x_{le} \geqq 1\right) \\
B(L^*,N^*) &= 0 && \left(L^* - x_{te} \geqq 1\right) \\
B(L^*,N^*) &= 1 - \left(L^* - x_{te}\right) && \left(0 < L^* - x_{te} < 1\right) \\
B(L^*,N^*) &= 1 && \left(L^* - x_{te} \leqq 0\right)
\end{aligned}\right\} \tag{15}$$

Wing total lift, drag, and pitching-moment coefficients are obtained by spanwise summations of the section data.

$$C_L = \frac{1}{\beta S} \sum_{N^*=N_{min}}^{N^*=N_{max}} c_l c \tag{16}$$

$$C_D = \frac{1}{\beta S} \sum_{N^*=N_{min}}^{N^*=N_{max}} c_d c \tag{17}$$

$$C_m = \frac{1}{\beta S l} \sum_{N^*=N_{min}}^{N^*=N_{max}} c_m c^2 \tag{18}$$

The wing area used in the expressions for the aerodynamic coefficients may be found through a summation

$$S = \frac{1}{\beta} \sum_{N^*=N_{min}}^{N^*=N_{max}} \sum_{L^*=1+[x_{le}]}^{L^*=1+[x_{te}]} A(L^*,N^*)\ B(L^*,N^*) \tag{19}$$

Optimum Combination of Loadings

Lagrange's method of undetermined multipliers has been applied in reference 3 to the problem of selecting a combination of component loadings yielding a minimum drag for a given lift. The method may be used for wings of any planform, provided that the interference drag coefficients are first determined. By using the nomenclature of the present report, the drag coefficient of the interference between any two loadings i,j may be expressed as:

$$C_{D,ij} = C_{D,ji} = \frac{1}{\beta S} \sum_{N^*=N_{min}}^{N^*=N_{max}} \sum_{L^*=1+[x_{le}]}^{L^*=1+[x_{te}]} \Delta C_{p,i}(L^*,N^*) \left(\frac{\partial z}{\partial x}\right)_j (L^*,N^*)\ A(L^*,N^*)\ B(L^*,N^*)$$

$$+ \frac{1}{\beta S} \sum_{N^*=N_{min}}^{N^*=N_{max}} \sum_{L^*=1+[x_{le}]}^{L^*=1+[x_{te}]} \Delta C_{p,j}(L^*,N^*) \left(\frac{\partial z}{\partial x}\right)_i (L^*,N^*)\ A(L^*,N^*)\ B(L^*,N^*) \tag{20}$$

and may be evaluated as an extension of the present numerical system.

The set of equations which establish the relative strength of each loading is

$$\left.\begin{aligned}
&C_{D,11}A_1 + C_{D,12}A_2 + C_{D,13}A_3 + \ldots + C_{D,1n}A_n + \lambda C_{L,1} = 0 \\
&C_{D,21}A_1 + C_{D,22}A_2 + C_{D,23}A_3 + \ldots + C_{D,2n}A_n + \lambda C_{L,2} = 0 \\
&C_{D,31}A_1 + C_{D,32}A_2 + C_{D,33}A_3 + \ldots + C_{D,3n}A_n + \lambda C_{L,3} = 0 \\
&\quad\vdots \qquad\quad \vdots \qquad\quad \vdots \qquad\quad \vdots \qquad\quad \vdots \\
&C_{D,n1}A_1 + C_{D,n2}A_2 + C_{D,n3}A_3 + \ldots + C_{D,nn}A_n + \lambda C_{L,n} = 0 \\
&C_{L,1}A_1 + C_{L,2}A_2 + C_{L,3}A_3 + \ldots + C_{L,n}A_n = C_L
\end{aligned}\right\} \tag{21}$$

Machine computing techniques allow the evaluation of the weighting factors A_i and thus the camber surface for an optimum combination of preselected loadings may be determined

$$z_c(x,y) = z_{c,1}(x,y)\ A_1 + z_{c,2}(x,y)\ A_2 + z_{c,3}(x,y)\ A_3 \ldots + z_{c,n}(x,y)\ A_n \tag{22}$$

The corresponding drag coefficient is

$$C_D = \frac{1}{2}\left(C_{D,11}A_1^2 + C_{D,12}A_1A_2 + C_{D,13}A_1A_3 + \cdots + C_{D,1n}A_1A_n + C_{D,21}A_2A_1 + C_{D,22}A_2^2 + C_{D,23}A_2A_3 + \cdots + C_{D,2n}A_2A_n + C_{D,31}A_3A_1 + C_{D,32}A_3A_2 + C_{D,33}A_3^2 + \cdots + C_{D,3n}A_3A_n + \cdots + C_{D,n1}A_nA_1 + C_{D,n2}A_nA_2 + C_{D,n3}A_nA_3 + \cdots + C_{D,nn}A_n^2\right) \quad (23)$$

Illustrative Examples

For a series of examples, the numerical method has been applied in obtaining camber surfaces for wings of various planforms and loadings. These results are useful in establishing the validity and accuracy of the method and in pointing out certain features of wings with curved or cranked leading edges.

The first example treats a delta-wing planform and an imposed pressure distribution identical with that of example II of reference 2. Thus, for the limiting case of straight-line leading and trailing edges, a comparison may be made of the results of the present numerical method and a more rigorous method. Figure 4 shows the wing planform and the imposed pressure distribution. Figure 5 shows the resultant camber surface shape as evaluated by a digital computer

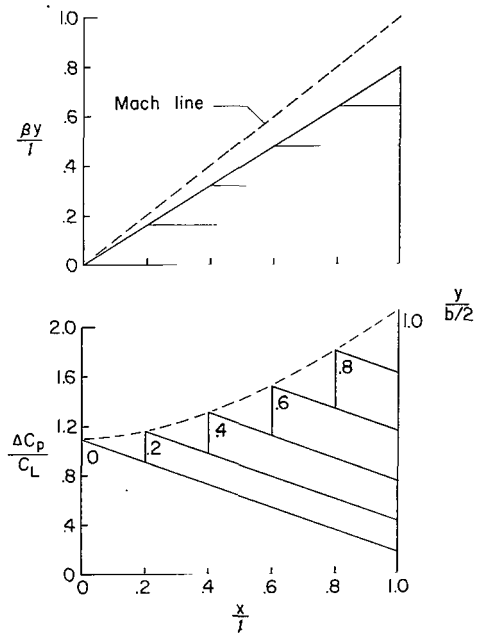

Figure 4.- Planform and pressure distribution for wing of example 1.

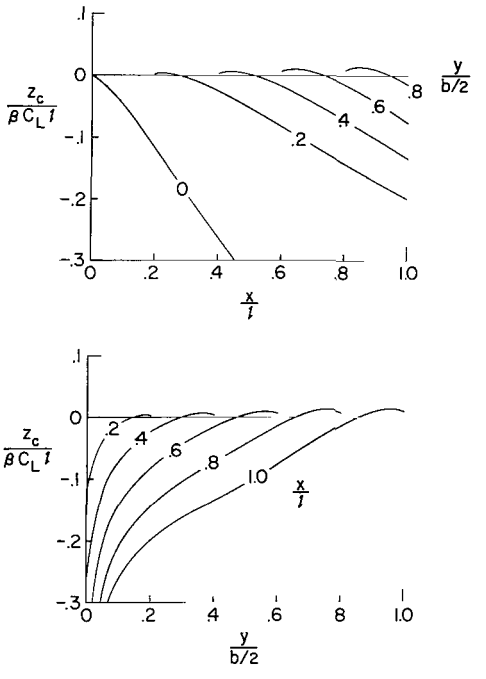

Figure 5.- Camber surface for wing of example 1. Camber ordinates adjusted to give a wing leading edge coincident with that for example II of reference 2.

program utilizing equations (8), (9), (10), and (11). The numerical method presented herein does not evaluate the upwash field ahead of the wing leading edge as does the method of reference 2. Thus to make these results directly comparable with the results of reference 2, the ordinates of figure 5 were modified through the addition of a set of incremental z_c values to make the leading edges coincident. Camber surface ordinates as in figure 5 may be shown in parametric form, since z_c is directly proportional to the wing length, the lift coefficient, and the Mach number term β. These results apply for a range of Mach numbers and planforms, provided that y_{le} and y_{te} are proportional to $1/\beta$. Note in figure 6 that near the midspan the wing camber surface takes on increasingly large negative values. This condition occurs because at $y = 0$ the integral of equation (1) is not convergent. This singularity at $y = 0$ does not invalidate the results for the major outboard area of the wing span.

A comparison of the wing trailing-edge ordinates defined by the numerical method (modified to give leading-edge coincidence) with the results of example II of reference 2 is made in figure 6. Generally good agreement is shown, and a well-pronounced tendency toward better agreement as the number of wing elements is increased may be observed. The wing planform as used in the program had a semispan of 40 units and a length of 50 units. Computing time with a Langley Research Center computer program averages less than 5 minutes for wings using this number of elements.

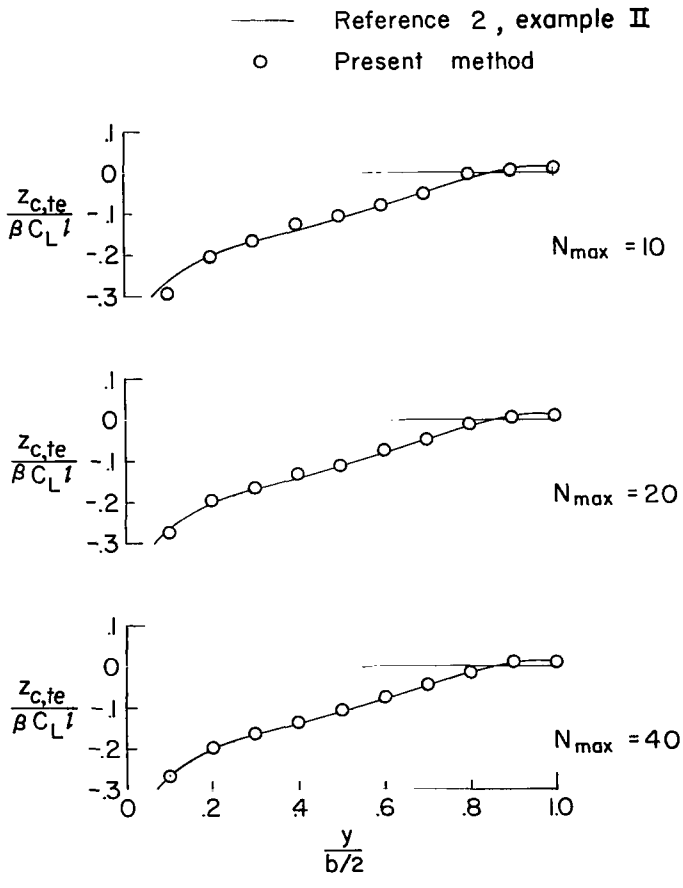

Figure 6.- Trailing-edge camber line for wing of example 1 compared with results for example II of reference 2.

An optimum combination of loadings for an "Ogee" type planform is treated in the second example. The wing planform and three selected component loadings are illustrated in figure 7. Camber surfaces corresponding to each of the loadings are shown in figures 8, 9, and 10. In the vicinity of $y = 0$ the same type of singularity appears as in the first example. Loadings a and c give a negative singularity, and loading b with ΔC_p proportional to $|y|$ gives a positive singularity.

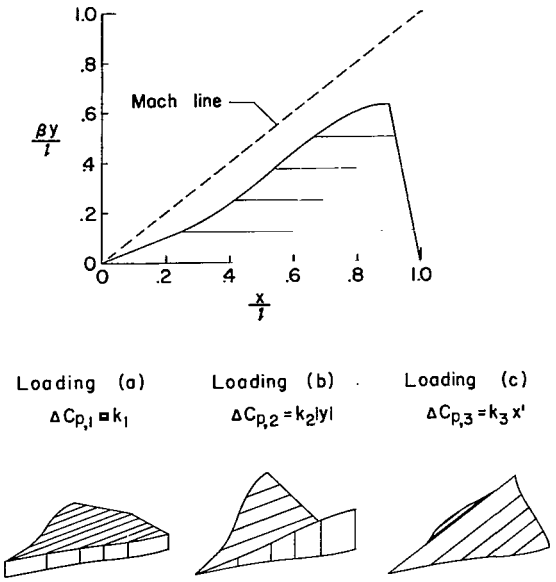

Figure 7.- Planform and component loadings for wing of example 2.

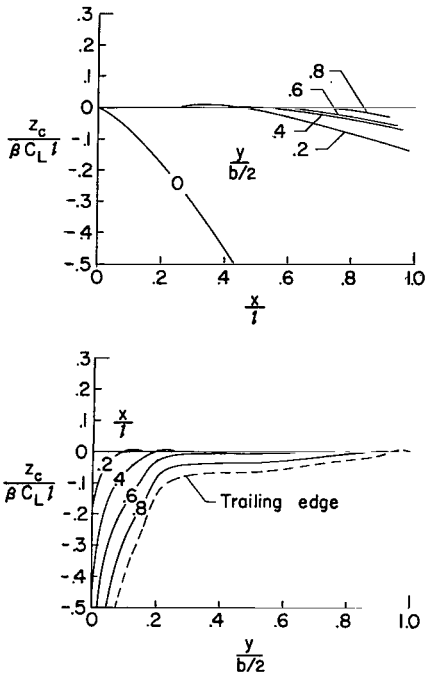

Figure 8.- Camber surface for wing of example 2 with component loading (a), $\Delta C_{p,1} = k_1$.

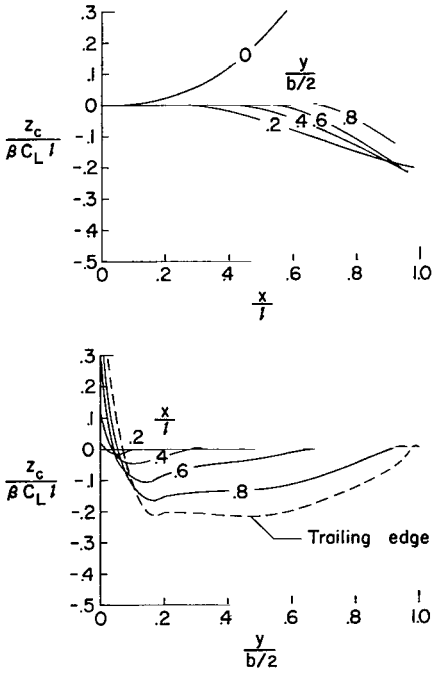

Figure 9.- Camber surface for wing of example 2 with component loading (b), $\Delta C_{p,2} = k_2|y|$.

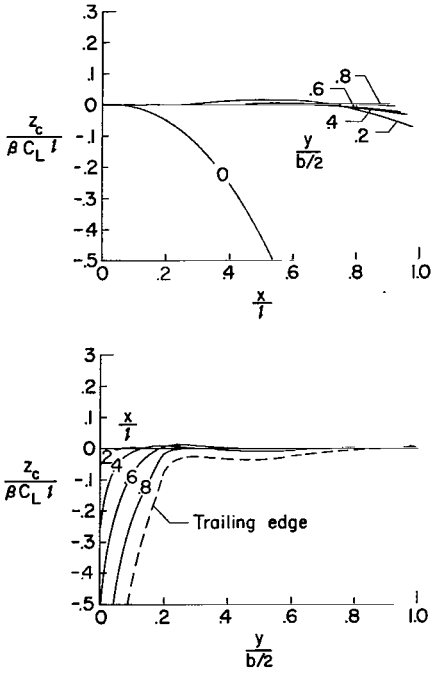

Figure 10.- Camber surface for wing of example 2 with component loading (c), $\Delta C_{p,3} = k_3 x'$.

The drag coefficients of the interference between pairs of loadings computed through use of equation (19) are as follows:

$$\frac{C_{D,11}}{\beta C_{L,1}^2} = 0.556 \qquad \frac{C_{D,12}}{\beta C_{L,1} C_{L,2}} = 0.406 \qquad \frac{C_{D,13}}{\beta C_{L,1} C_{L,3}} = 0.700$$

$$\frac{C_{D,22}}{\beta C_{L,2}^2} = 0.821 \qquad \frac{C_{D,23}}{\beta C_{L,2} C_{L,3}} = 0.254 \qquad \frac{C_{D,33}}{\beta C_{L,3}^2} = 1.100$$

Solution of equation (20) yields the following values of the loading factors

$$A_1 = \frac{1.697}{C_{L,1}} \qquad A_2 = \frac{-0.067}{C_{L,2}} \qquad A_3 = \frac{-0.630}{C_{L,3}}$$

which define an optimum pressure distribution derived from the three-component loadings which may be expressed as

$$\frac{\Delta C_p}{C_L} = 1.697 - 0.188\frac{|y|}{b/2} - 2.04\,\frac{x'}{l}$$

The camber surface corresponding to this optimum loading was determined through a repetition of the basic program. This resultant wing whose camber surface is shown in figure 11 has a drag-due-to-lift factor $C_D/\beta C_L^2$ of 0.238. Since drag-due-to-lift characteristics for an uncambered wing of this planform are not known, the drag reduction due to camber can not be evaluated. However, it may be seen that this relatively low drag is due to camber rather than to planform, since an optimum camber delta wing of the same aspect ratio would have a drag-due-to-lift factor of about 0.22 compared to about 0.32 for the corresponding flat-plate delta wing. A Langley Research Center computer program which determines an optimum combination of three loadings and computes the resultant wing shape required about 25 minutes for the solution of the problem.

The final set of examples illustrates the strong influence of leading-edge planform shape on the camber surface required to support specified loading distributions. The reference arrow wing (example 3) and its restricted optimum loading distribution described in some detail in reference 4 is shown in figure 12. The camber surface, resulting from the machine computation is shown in figure 13. A numerical integration of the imposed loading over this surface yields a drag-due-to-lift factor $C_D/\beta C_L^2$ of 0.169, about 4 percent less than that of the analytic solution following the method of reference 2. This discrepancy is due in large part to the fact that the numerical solution gives finite values of the surface gradients at the root chord rather than the infinities of the analytic solution. An enlarged grid system would provide better correlation. The drag-due-to-lift factor for the corresponding flat-plate arrow wing without leading-edge suction is 0.288.

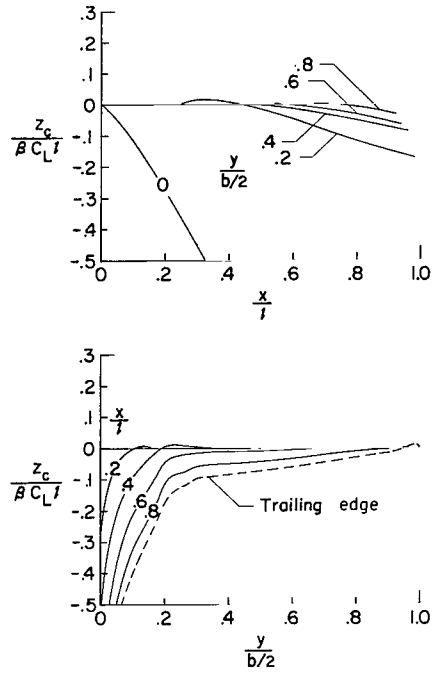

Figure 11.- Camber surface for wing of example 2 with optimum combination of component loadings.

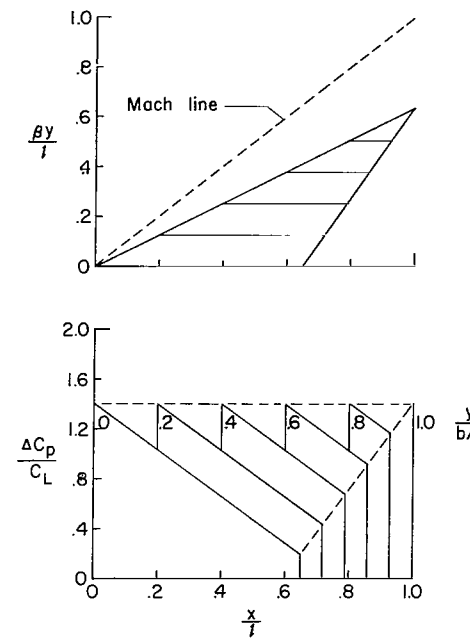

Figure 12.- Planform and pressure distribution for wing of example 3.

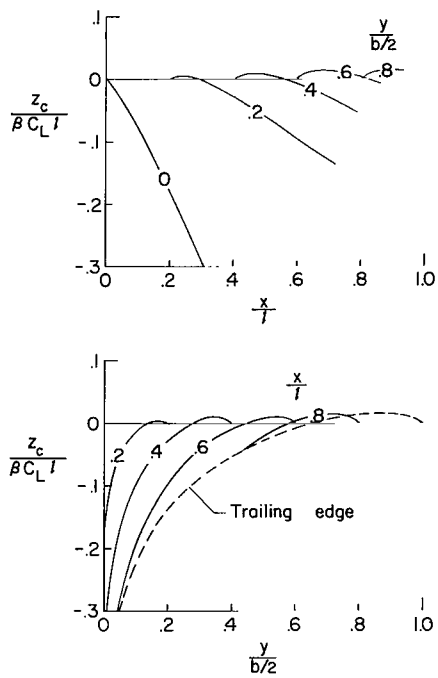

Figure 13.- Camber surface for wing of example 3.

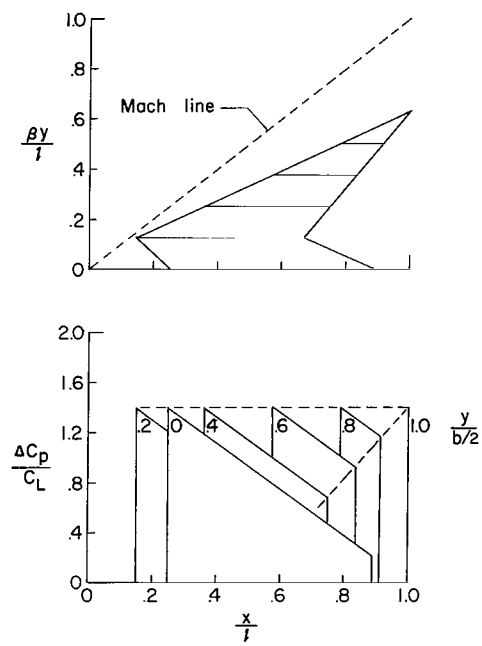

Figure 14.- Planform and pressure distribution for wing of example 4.

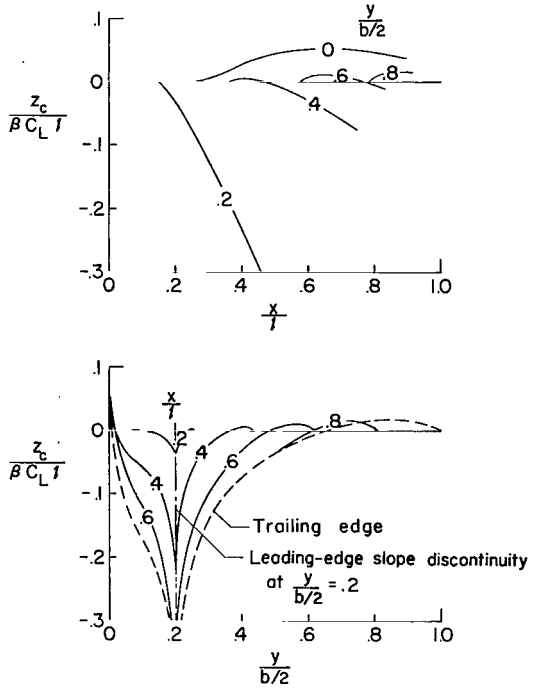

Figure 15.- Camber surface for wing of example 4.

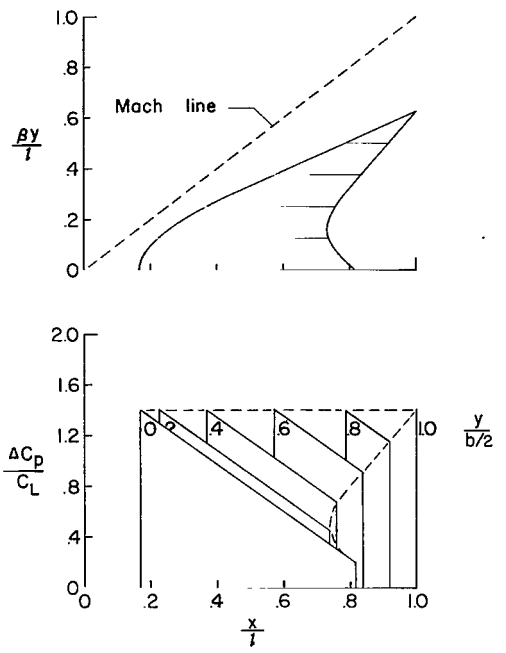

Figure 16.- Planform and pressure distribution for wing of example 5.

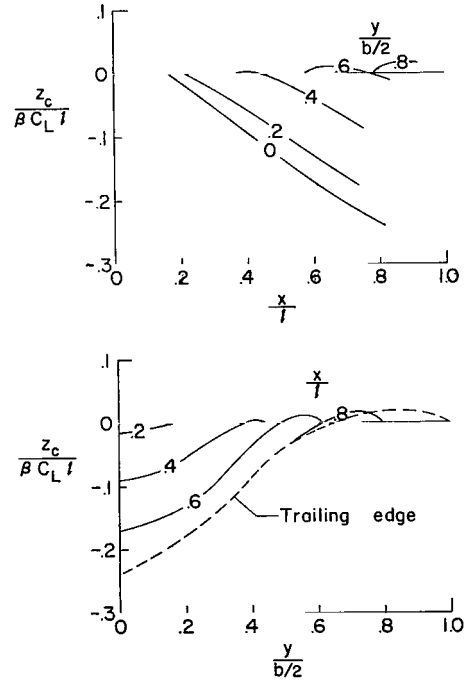

Figure 17.- Camber surface for wing of example 5.

In figure 14 is shown the planform of an M wing (example 4) which has the same spanwise chord distribution as the arrow wing. The pressure distribution is similar to that of the arrow wing in that the spanwise load distribution is preserved. The resultant surface shape (fig. 15) for this planform and load distribution requires large local angles of attack directly behind the leading-edge break at $\frac{y}{b/2} = 0.2$. The drag-due-to-lift factor for the wing is 0.228.

A curved-leading-edge wing (example 5) with its load distribution is shown in figure 16. Again the spanwise chord distribution and the spanwise loading distribution are preserved. As shown in figure 17, the rounded apex of this wing planform combined with the chosen pressure distribution results in finite values of z_c at $y = 0$. The drag-due-to-lift factor of 0.195 is 15 percent higher than that for the warped arrow wing; however, since severe camber is not required, that value may be more easily attainable in practice.

CONCLUDING REMARKS

A numerical design method which allows the determination of camber surfaces corresponding to certain specified load distributions on wings of arbitrary planform has been presented. It has been illustrated how these results may be combined with existing methods of selecting optimum combinations of loadings. Application of the method was illustrated in a series of examples which served to establish its precision and also served to point out certain features of wings with curved or cranked leading edges.

Langley Research Center,
National Aeronautics and Space Administration,
Langley Station, Hampton, Va., March 13, 1964.

REFERENCES

1. Brown, Clinton E., and McLean, Francis E.: The Problem of Obtaining High Lift-Drag Ratios at Supersonic Speeds. Jour. Aero/Space Sci., vol. 26, no. 5, May 1959, pp. 298-302.

2. Tucker, Warren A.: A Method for the Design of Sweptback Wings Warped To Produce Specified Flight Characteristics at Supersonic Speeds. NACA Rep. 1226, 1955. (Supersedes NACA RM L51F08.)

3. Grant, Frederick C.: The Proper Combination of Lift Loadings for Least Drag on a Supersonic Wing. NACA Rep. 1275, 1956. (Supersedes NACA TN 3533.)

4. Carlson, Harry W.: Aerodynamic Characteristics at Mach Number 2.05 of a Series of Highly Swept Arrow Wings Employing Various Degrees of Twist and Camber. NASA TM X-332, 1960.

5. McLean, F. Edward, and Fuller, Dennis E.: Supersonic Aerodynamic Characteristics of Some Simplified and Complex Aircraft Configurations Which Employ Highly Swept Twisted-and-Cambered Arrow-Wing Planforms. Vehicle Design and Propulsion. American Inst. Aero. and Astronautics, Nov. 1963, pp. 98-103.

6. Lomax, Harvard, Heaslet, Max A., and Fuller, Franklyn B.: Integrals and Integral Equations in Linearized Wing Theory. NACA Rep. 1054, 1951. (Supersedes NACA TN 2252.)

7. Mangler, K. W.: Improper Integrals in Theoretical Aerodynamics. Rep. No. Aero. 2424, British R.A.E., June 1951.

2/7/85

"The aeronautical and space activities of the United States shall be conducted so as to contribute . . . to the expansion of human knowledge of phenomena in the atmosphere and space. The Administration shall provide for the widest practicable and appropriate dissemination of information concerning its activities and the results thereof."

—NATIONAL AERONAUTICS AND SPACE ACT OF 1958

NASA SCIENTIFIC AND TECHNICAL PUBLICATIONS

TECHNICAL REPORTS: Scientific and technical information considered important, complete, and a lasting contribution to existing knowledge.

TECHNICAL NOTES: Information less broad in scope but nevertheless of importance as a contribution to existing knowledge.

TECHNICAL MEMORANDUMS: Information receiving limited distribution because of preliminary data, security classification, or other reasons.

CONTRACTOR REPORTS: Technical information generated in connection with a NASA contract or grant and released under NASA auspices.

TECHNICAL TRANSLATIONS: Information published in a foreign language considered to merit NASA distribution in English.

TECHNICAL REPRINTS: Information derived from NASA activities and initially published in the form of journal articles.

SPECIAL PUBLICATIONS: Information derived from or of value to NASA activities but not necessarily reporting the results of individual NASA-programmed scientific efforts. Publications include conference proceedings, monographs, data compilations, handbooks, sourcebooks, and special bibliographies.

Details on the availability of these publications may be obtained from:

SCIENTIFIC AND TECHNICAL INFORMATION DIVISION

NATIONAL AERONAUTICS AND SPACE ADMINISTRATION

Washington, D.C. 20546